

The role of thermal coupling on avalanches in manganites

This article has been downloaded from IOPscience. Please scroll down to see the full text article.

2009 J. Phys.: Condens. Matter 21 406005

(<http://iopscience.iop.org/0953-8984/21/40/406005>)

View [the table of contents for this issue](#), or go to the [journal homepage](#) for more

Download details:

IP Address: 129.252.86.83

The article was downloaded on 30/05/2010 at 05:32

Please note that [terms and conditions apply](#).

The role of thermal coupling on avalanches in manganites

F Macià, G Abril, J M Hernandez and J Tejada

Departament de Física Fonamental, Facultat de Física, Universitat de Barcelona—Avinguda Diagonal 647, Planta 4, Edifici nou, 08028 Barcelona, Spain

Received 18 June 2009, in final form 27 August 2009

Published 14 September 2009

Online at stacks.iop.org/JPhysCM/21/406005

Abstract

We report here a study on the environmental dependence of the occurrence, at low temperature, of ultra-sharp field induced avalanches in phase separated manganites. Despite the high reproducibility of avalanches, it has already been observed that the critical fields shift with the magnetic field sweep rate and that different sample sizes lead to different ignition fields for the avalanches. Critical growing rates have been suggested to describe the avalanche ignition though the role of thermal coupling has hardly been considered. We qualitatively analyze here a set of experimental data on avalanches in manganites and discuss the role of thermal coupling as a key parameter of the instability in a dynamical system.

(Some figures in this article are in colour only in the electronic version)

1. Introduction

$\text{La}_{5/8-y}\text{Pr}_y\text{Ca}_{3/8}\text{MnO}_3$, LPCMO(y) manganites show a fascinating and widespread set of properties connecting spins with electrical charges and their spatial and geometrical arrangements. One of the most interesting points is the coexistence below a certain temperature, $T_C \sim 100$ K, of phase separated (PS) states; charge disordered ferromagnetic (CD-FM) and charge ordered antiferromagnetic (CO-AFM) [1–3]. Moreover, the phase separated state could be dynamic. The phase concentration of CD-FM and CO-AFM continuously changes with temperature and magnetic field. After zero field cooling (ZFC) the system is blocked in a metastable state with a predominance of the CO-AFM insulating phase, strongly depending on the Pr content, y . An increase in temperature or the applied magnetic field promotes the dynamics and CD-FM domains grow over the AFM phase until it becomes completely dynamic and the CD-FM phase becomes the majority of the sample. The surprising property that has been recently found in some phase separated manganites is the abrupt and rapid phase change of the entire sample from the CO-AFM phase to the CD-FM [4–8] that takes place at low temperatures under the effect of fast sweeping magnetic fields. The phase avalanches correspond to a front propagating through the sample and the whole process lasts, at most, a few milliseconds [9, 10]. This rapid phase transition is also responsible of the spectacular effect of the colossal magnetoresistance (CMR) [11–14]. It is also to be noted that such transitions of the entire sample

from one phase to the other are included in the category of metamagnetic transitions [15].

Avalanches in LPCMO(y) manganites are processes involving heat propagation [3, 10], as are those reported on molecule magnets [16, 17] and, probably, as are many other reported physical transitions showing steps in isothermal magnetization curves [18], often called *step-like* [19, 20], *staircase* [21] or *abrupt jumps* [5, 9]. The statements ‘appear when the sample is large enough’ or ‘take place under fast magnetic field sweep rates’ has been widely used to refer to the particular conditions under which the avalanches used to occur [22, 23]. It is completely accepted that all kinds of avalanche ignition are basically instability processes. Small perturbations could drive systems to either a total change or to nothing. A subtle noise hardly perturbs the snows of a high mountain, but in some cases it turns to be drastic. When approaching a match flame to a piece of paper, the paper is ignited in the very moment the distance to the flame is ‘say d ’, however, if the flame is kept slightly farther than d the paper never ignites. Furthermore, under certain circumstances it is possible to have the paper burn with no flame, slow burning. In more ‘condensed matter’ terms, when a system is blocked in a metastable state with an effective barrier separating that state from the lower energy state, a small perturbation or a quick variation of the conditions thermally activates a portion of the material that relaxes, overcoming the barrier and releasing energy that could, in principle, be reabsorbed by the rest of the material and used to overcome the barrier again, and so on. In

practice, though the coupling with the environment needs to be considered. There is a competing energy balance between the released energy because of the difference between the energy of the states and the absorbed energy by the environment. A magnetic avalanche deals with the same physics as a magnetic slow relaxation, the main difference is that in a slow relaxation the sample is supposed to be thermalized at every moment.

Ghivelder *et al* [5] pointed out the released energy during the phase transition and the subsequent increase in temperature as key points in understanding the dynamical process of phase avalanches. There are some reported experiments studying transition steps on perovskite manganites that can be currently described in terms of heat propagation and the related discussions probably reviewed within a thermal coupling frame [19, 21, 9]. Direct evidence, on other materials, of the importance of the thermal coupling when dealing with avalanches involving heat processes [24] have been reported. We analyze in this paper the dynamics of the abrupt phase transition, at low temperature, from the CO-AFM to the CD-FM state in samples of $\text{La}_{5/8-y}\text{Pr}_y\text{Ca}_{3/8}\text{MnO}_3$ focusing on the effect of the bath coupling on the appearance of the phenomenon.

2. Experimental details

We studied several polycrystalline samples of composition $\text{LPCMO}(y)$ ($y = 0.40, 0.38$ and 0.36) with different dimensions and under different bath couplings. The samples were placed in the bore of a commercial superconducting magnet system (PPMS Quantum Design) in a sealed sample chamber. The system is capable of producing magnetic fields up to 5 T and temperatures in the range of 300–2 K. All samples were characterized by measuring the temperature dependence of the magnetization, all showing the same values for the ferromagnetic transition (between 50 and 70 K on cooling and between 80 and 100 K on warming, under 1 T) and the blocking temperature at about 25 K under 1 T [3, 25].

3. Instability model

Let us here model the dynamical system describing the evolution of the FM phase fraction, x , at a finite temperature. At the beginning, after zero field cooling the sample, there is a predominant CO phase blocked. As either the magnetic field or the temperature increases, the CO clusters are more likely to overcome a barrier $U(H, x)$ separating the two phase states. During the relaxing process an exponentially small number of molecules will react and release heat (as the FM phase has lower energy than the CO). The heat will flow out of the sample, creating a steady and smooth temperature profile along the substance, with a slightly higher temperature in the bulk compared to the temperature at the surface, T_0 .

At low temperatures, below the blocking temperatures, large samples of $\text{LPCMO}(0.40)$ systematically show avalanches when sweeping the magnetic field from zero to a large positive value. The metastability (i.e., most of the sample is made of the CO phase) is suddenly broken at a particular point of the bias field and the whole sample becomes FM.

However, there are some conditions under which no avalanches are detected namely, small crystals, slow sweeping fields, high well bath coupling, among others.

To understand the ignition process of avalanches we should consider basically two processes involving heat. The first one is related to the transport along the sample, $C\dot{T} = \nabla \cdot k\nabla T$ where k is the thermal conductivity and C the heat capacity. The other involved thermal phenomenon is the energy released by the phase transition, which is basically given by $\Delta E = u_{\text{CO}} - u_{\text{FM}} > 0$. When this energy is thermalized it leads to a change in temperature $C\Delta T = \Delta E$. Let us consider a simple equation to describe the FM phase fraction dynamics [3], \dot{x} , from the initial state x_i to the final $x_{\text{eq}} > x_i$ state, $\dot{x} = \frac{(x_{\text{eq}} - x)}{|x_{\text{eq}} - x|} \Gamma$, where $\Gamma = \Gamma_0 \exp[-\frac{U}{T|x_{\text{eq}} - x|}]$ with Γ_0 a fixed relaxation rate. The complete equation system describing both temperature and FM phase fraction evolution in the sample can be written as a reaction–diffusion system for the temperature,

$$\begin{aligned} C\dot{T} &= \dot{x}\Delta E + \nabla \cdot k\nabla T \\ \dot{x} &= \Gamma_0 \exp\left[-\frac{U}{T(x_{\text{eq}} - x)}\right], \end{aligned} \quad (1)$$

where we have assumed $x < x_{\text{eq}}$ and we are just worried about the dynamics of x towards x_{eq} , being the equilibrium state where the sample is completely made of the FM phase.

The coupling with the bath and the sample geometry should be considered; both are actually the reason that small crystals do not show avalanches or that sweeping fields affect the ignition process. Boundary conditions must therefore be added to equations (1).

It is accepted that avalanches are related to the instability of smooth temperature profiles when the FM phase grows against the existing CO phase. Our study here is based on a linear stability analysis of the system of equations (1).

To perform a linear stability analysis requires elimination of the spatial dependence of equations (1). Let us assume that the magnetic field and temperature of the sample are independent of the coordinates and the boundary is fixed at a temperature $T = T_0$. The dissipation term in the equation for the temperature evolution has to be modified; we consider the thermal diffusivity, $\kappa = k/C$, does not change in the vicinity of T_0 and thus $\Gamma_d = \frac{2\kappa_0}{R^2}$ is the rate of thermal equilibration within the sample close to $T = T_0$ and κ_0 is the thermal diffusivity at $T = T_0$. R is the distance from the center of the sample ($l = 2R$ is a characteristic length of the order of the smallest dimension of the sample). Notice that, considering a sample in thermal contact with the environment and assuming the boundary is fixed at $T = T_0$, we force the thermal diffusivity κ to depend on the effective bath coupling (i.e., only with no environment we could recover κ as the real thermal diffusivity of the sample), thus the equilibration Γ_d involves both heat conduction properties of the sample, dimensionality and coupling with the bath.

Additionally, as we focus on the instability at the very beginning, and not in the further propagation, we can assume the variation of the FM phase fraction, x , hardly changes, being

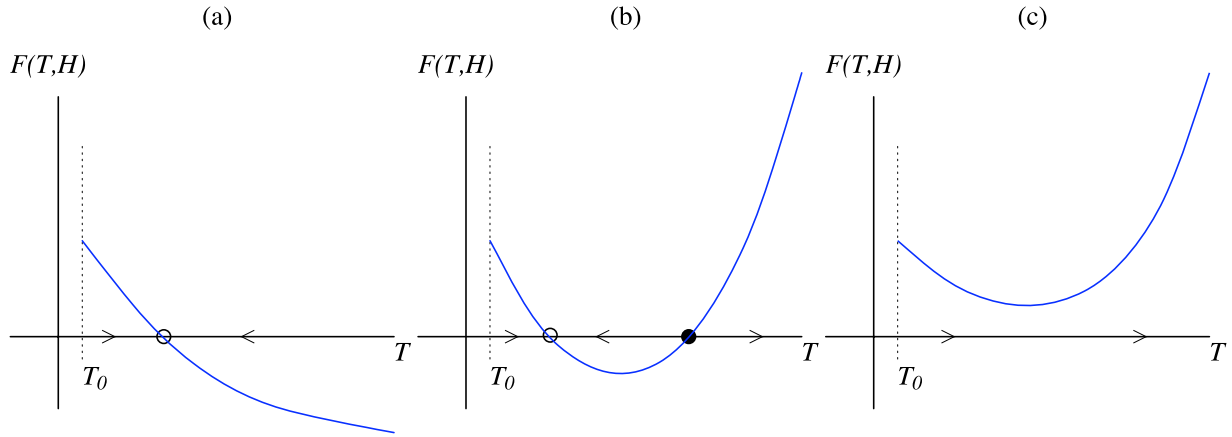


Figure 1. Diagrams of stability for $F(T, H) = \dot{T}$. In (a) there is one stable critical point, in (b) there are two critical points, the first one is stable and the second one is unstable and in (c) there are no critical points.

x_b the initial FM fraction available for experiencing the fast transition, $x_b = x_{eq} - x_i$.

The above considerations lead to a new equation for the temperature evolution.

$$\dot{T} = \frac{\Delta E}{C} \Gamma_0 \exp\left[-\frac{U}{Tx_b}\right] - \Gamma_d(T - T_0) = F(T, H). \quad (2)$$

The stationary solutions (critical points, $\dot{T} = 0$) for this equation correspond to those temperatures at which the dissipation term equals the released energy. A first glance at the function $F(T, H)$ lets us know that assuming the initial temperature, the bath temperature $T = T_0$, the function $F(T_0, H)$ is positive, indicating an upward trend for the temperature at the beginning of the process (the growth of the FM phase releases heat).

The function $F(T, H)$ at a fixed ΔE (i.e., at a fixed applied magnetic field) has a negative dissipating term increasing linearly with temperature, whereas the reaction term increases exponentially for low T . There is a competition between these two terms. The function $F(T, H)$ can be basically classified in three different cases depending on whether it has zero, one, two zeros (i.e., critical points, $\dot{T} = 0$); figure 1 shows both cases. Just one zero (see figure 1(a)) indicates the dissipating term always dominates against the reaction at temperatures above the critical point, which is therefore stable, and consequently there is a steady relaxation at constant T at $\dot{T} = 0$ ($\partial_T F(T, H) < 0$). The second case to describe is when the $F(T, H)$ has two zeros (see figure 1(b)), the dissipating term only dominates in a short temperature range above the first critical point. In that case, there is second critical point which is unstable ($\partial_T F(T, H) > 0$) (notice that this point can only be reached with the help of a heater that supplies the necessary energy). In the third case the reaction term is always larger than the dissipation and consequently there are no stable points at \dot{T} see figure 1(c). This last case leads to the ignition of an avalanche.

As the magnetic field increases (the energy difference between the two phases becomes larger), the reaction term also increases as long as the initial fraction x_b remains constant.

Therefore, assuming a diagram as in figure 1(b), the two critical points, $\dot{T} = 0$, would get closer one to each other until they disappear. At that very field there would be no more stable solutions for equation (2) and the \dot{T} will be positive at all temperatures. Consequently, the temperature would rise exponentially. Such a situation can be defined as a *spontaneous avalanche*. On the other hand, avalanches can also be ignited providing there is a sufficient quantity of energy to reach the second critical point (the unstable one) of equation (2). Such induced avalanches were first performed in molecule magnets [17, 26, 27] by introducing the use of surface acoustic waves or simply heaters in order to rapidly raise the temperature of the sample. Acoustic waves have been also used to ignite avalanches in LPCMO manganites [10] and study the time duration as a function of the applied magnetic field.

One of the basic requirements to have avalanches is therefore that both terms in equation (2) must be comparable. We have already emphasized the dependencies of the dissipating term, $\Gamma_d = \frac{\kappa_0}{R^2}$; it increases with both the heat conduction properties of the sample and the bath coupling, and decreases with the sample size. On the other hand, the reaction term increases with temperature and with a tilting of the energy difference between the two states (i.e., ΔE increases). However, the most important point in the reaction term is how far the system is from the equilibrium; there is a strong dependence on the available AFM phase fraction to burn, $x_b = x - x_{eq}$.

Thus, once we have a sample with comparable dissipation and reaction terms (similar to figure 1(b)) it is then possible to ignite avalanches by supplying enough energy to the sample to reach the instability. Spontaneous avalanches can be obtained by sweeping the magnetic field and driving the system out of equilibrium. However, slow sweeping fields would not produce avalanches because the increase of released energy is compensated for by the variation of the initial FM state. Fast sweeping fields, however, would not allow the sample to relax, and having the same initial FM concentration the reaction term will increase until the instability is reached.

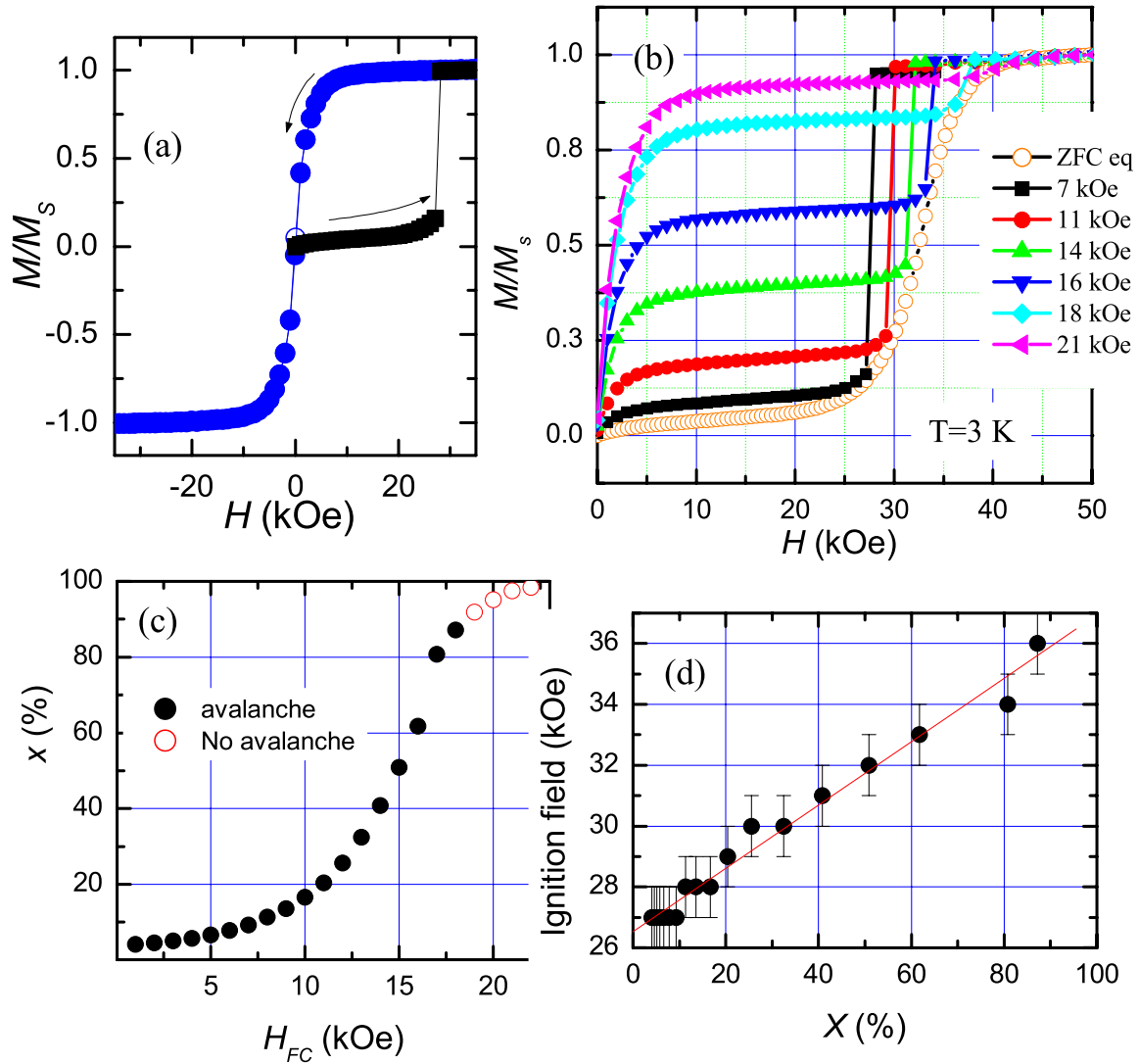


Figure 2. (a) The field dependence of the magnetization at 3 K. Squares correspond to the first magnetization curve after ZFC, whereas circles show the magnetic measurements from 35 to -35 kOe and back to 35 kOe. (b) Isothermal magnetization curves at $T = 2.5$ K, after field cooling the sample (LPCMO(0.4)). Black squares correspond to the zero field cooled process whereas magenta left triangles correspond to the case when the sample was cooled under $H_{FC} = 20$ kOe. (c) The values for x reached as a function of the field cooling, with a fixed cooling rate of 10 K min^{-1} . (d) Critical field dependence on the initial ferromagnetic concentration x .

4. Results and discussion

In order to produce controlled and reproducible avalanches, we first performed the field cooling process of the sample at a constant cooling rate down to the lowest desired temperature between 2 and 4 K. This process allows us to control the concentration, x , of the CD-FM phase before starting the field sweep. The concentration, x , of each sample is fully determined by the cooling rate and the value of the external applied magnetic field during the cooling process [10] (this concentration depends on the Pr content, y , and it has been recently shown that it is also affected by the value of internal microstrains [28]). Figure 2(c) shows the values of reached x reached at low temperature for different field cooling processes with a fixed cooling rate of 10 K min^{-1} . In the case of the zero field cooling process the x value was lower than 7%, indicating that the sample was mainly in the CO-AFM

phase. Figure 2(a) shows the isothermal magnetization curve measured at 3 K after ZFC for a sample LPCMO(0.4) with $M_s = 1.23 \text{ emu}$. In the first magnetization curve (squares) a magnetic avalanche was detected at $H = 28 \text{ kOe}$, the final magnetization (at 40 kOe) being the saturation value, M_s . The saturation value corresponds to the case of having the sample completely in the ferromagnetic phase, $x = 1$. We then kept the temperature constant and measured, immediately after, a $M(H)$ going from 35 kOe down to -35 kOe and back to 35 kOe (circles). This hysteresis cycle shows that the ferromagnetic state has neither remanence nor coercivity and, consequently, there are no time dependent phenomena. To repeat the process we need to have the sample warmed up to the reversibility temperature above 120 K and cooled down again. The avalanches are completely deterministic and totally reproducible. The value of x throughout the first magnetization curve, when the sample is still mostly the AFM

phase, can be estimated, at each temperature and magnetic field, from the ratio between M and the value of M at the same temperature and magnetic field of the ferromagnetic curve. The magnetization after magnetic avalanches always reaches the value corresponding to the saturation magnetization of the ferromagnetic phase, $x = 1$. It has been recently shown that the magnetic field values at which the avalanches appear are fully determined by the value of x [19, 10, 9]. Figure 2(b) shows a few isothermal curves measured after different field cooling processes (between 0 and 20 kOe) at a temperature of 2.5 K (the same sample LPCMO(0.4) was used). It is clear from figure 2(b) that, at fixed T , the value of the applied magnetic field, H_a , at which the avalanche spontaneously appears depend on the FM phase fraction, x . Moreover, this dependence is linear (see figure 2(d)). The different curves $M(H)$ in figure 2(b) correspond, therefore, to different initial blocked states, tuned by the cooling field. Once the avalanche was ignited, the CD-FM phase started to grow against the CO-AFM phase, resulting in heat that further accelerated the phase transition process [3, 10]. Both the ignition and the propagation through the sample of the spin reversing process are dominated by the rate of the heat delivered and the heat conduction through the sample [29]. Both processes are very sensitive to the phase fraction x_a [25].

Figure 3 (upper inset) shows isothermal magnetization curves with no avalanches (in LPCMO(0.4)). Data were registered at several temperatures between 3 and 5 K after zero field cooling the sample. Magnetic avalanches are turned on due to the interplay between the released heat, in the microscopic transformation when the local CD-FM phase fraction increases, and the absorption of that same released energy [3, 10]. To avoid the ignition of these avalanches we increased the number of points that were measured at the same interval of applied magnetic field with respect to the hysteresis curve of figure 2(a). As each point takes several seconds to be measured, this reduces the average sweep rate of the applied magnetic field, allowing the sample to thermalize and making possible to register the magnetization, M , values of the PS state at many different magnetic fields and temperatures, otherwise the sample would have already transited to the CD-FM state. Actually, more important than the averaged sweeping magnetic field are the smaller steps. Variations of the magnetic field drive the system out of equilibrium, and stopping the sweep so often makes the sample reach a blocked metastable state at every instant such that critical conditions do not appear. Values of the magnetization curves at magnetic fields smaller than 20 kOe perfectly coincide, indicating that the FM phase fraction, x , is nearly the same at all temperatures between 3 and 5 K (see upper inset of figure 3). On the other hand, at larger magnetic fields (above 20 kOe), there is a separation between the different temperature magnetization curves, indicating that the accessible CD-FM phase fraction depends on both the temperature and the magnetic field. We plotted those differences in the middle inset of figure 3. Time dependent phenomena occur in this range emphasizing that the phase separation is a dynamic process governed by an energy barrier functional, depending on H , T and x ($U(H, T, x)$) [25], that separates the CD-FM and the CO-AFM states. The changes

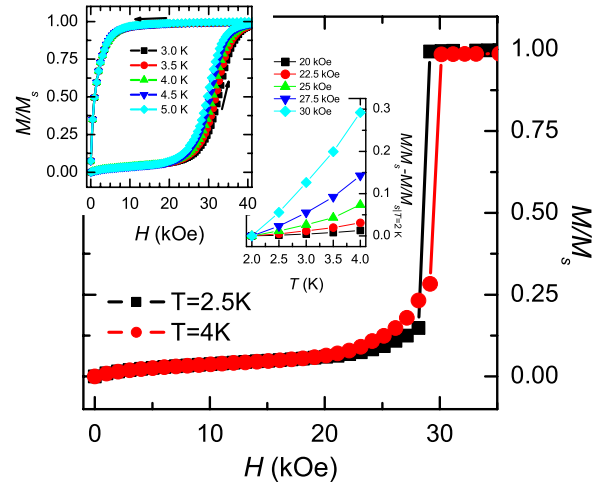


Figure 3. Avalanches in the isothermal curves at 2.5 K (black squares) and 4 K (blue circles) when the measurements were done with a spacing of 1000 Oe/step with a sweep rate of 300 Oe s⁻¹. The upper inset shows isothermal magnetization curves registered at several temperatures between 3 and 5 K after zero field cooling the sample. The curves were measured with a spacing of 500 Oe/step with a sweep rate of 300 Oe s⁻¹. The inset in the middle of the figure plots the difference between isothermal magnetization curves at different temperatures at 4 values of the magnetic field.

in x are therefore due to thermal transitions above this barrier height. Figure 3 shows isothermal magnetization curves at two different temperatures for a large sample of LPCMO(0.4) ($M_s = 1.23$ emu). The curves have been measured with a faster sweep field in order to produce avalanches. Similar to what we showed in figure 2(b), the field H_a shifts to higher values because the two temperatures made the sample relax differently before the appearance of the avalanche. The FM phase fraction of the sample with higher temperature evolved more quickly resulting in a large FM phase fraction, x , and, as in figure 2(b), finally leading to higher values of H_a .

In order to detect, and further study, the effects of the thermal coupling on the ignition of avalanches we performed several isothermal magnetization curves with different sweep rates. All other conditions were kept constant and the only difference between the curves in figure 4 were the applied magnetic field sweep rates. Actually, we just modified the number of measured points, the field spacing between DC magnetization measurements (e.g., we stopped the sweeping field a different number of times per curve and we measured the magnetization every time we stopped). One could expect a similar behavior to that which we found in figure 3, where at higher temperatures the FM phase grew quickly with the magnetic field and consequently avalanches appeared. Large samples were used (in figure 4(a) the same as in the inset of figure 3). We clearly observe that the FM phase fraction, x , is exactly the same through the whole field sweep. However, as the number of stops increased, the magnetic field H_a , where the avalanche appeared, shifted towards higher values and for the slower sweep rate there are no more avalanches. Earlier on, we saw there were time dependent phenomena above 20–25 kOe but now the different sweeping rates did

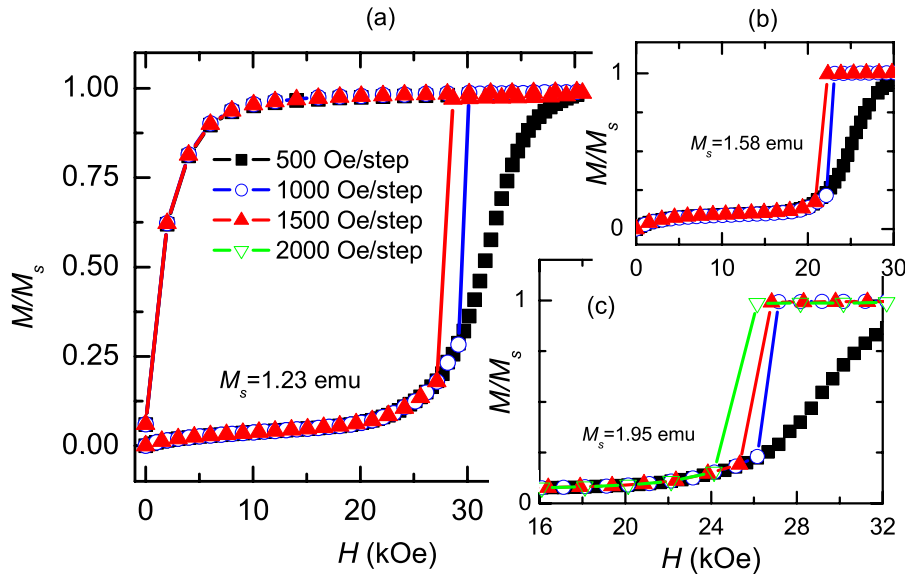


Figure 4. Isothermal magnetization curves measured with different sweeping magnetic fields (different spacing between measurements). 500 Oe/step with black squares, 1000 Oe/step with blue circles, 1500 Oe/step with red up-triangles and 2000 Oe/step with green down-triangles. The temperature was $T = 4$ K. In (a) LPCMO(0.4), in (b) LPCMO(0.38) and in (c) LPCMO(0.36)

not produce appreciable changes at large magnetic fields (see figure 4). The importance of the necessary conditions to get the instability that finally leads to avalanches should be highlighted. The experiment clearly shows the sweeping magnetic field is responsible for driving the system out of equilibrium; the higher the sweep rate, the lower the avalanche fields H_a . This effect has already been observed in other samples [21, 9, 7, 6, 8]. We suggest understanding the results in the frame of thermal coupling. It is obviously easier to drive our system out of equilibrium when the magnetic field is sweeping than waiting at a particular value of the field. In the first case, we add energy to the system which, in addition, will release more energy due to the phase transition. On the other hand, at a fixed value of the magnetic field, there is only the energy given by the relaxing clusters changing their phase. The same experiment was performed with samples of different composition (LPCMO(0.36) in figure 4(c) and LPCMO(0.38) in figure 4(b)) having very similar results. Samples with slightly different composition on y have different barrier heights, and consequently avalanches occur at different magnetic fields. We were interested in going further in that direction and proving not only that there are critical values of the sweeping field rate that drives the sample to instability but also define the particular role of the interplay with the thermal environment.

We performed, with the same sample, several isothermal magnetization curves at a fixed temperature by just changing the material of the sample holder. As the samples were, within the cryostat, surrounded by He_4 gas, they were supposed to considerably change their thermal coupling with the bath when changing the sample holder. We started with a sample on a plastic stand and we expected to have, in that case, a bad thermal coupling with the bath. The second holder was basically the same as the first one but it had a small 2 mm diameter copper wire directly in contact with the sample. The

third case consists of a sample totally wrapped with a 0.1 mm diameter copper wire. In both cases the sample had been zero field cooled at a fixed temperature rate of 10 K min^{-1} obtaining practically identical initial states. We can see in figure 5(a) how the magnetic field H_a varies in each case. The better the thermal coupling, the larger the threshold field, H_a . The energy difference between the two phase states increases with the applied magnetic field, therefore, the amount of released heat, due to the transition from the AFM phase to the FM phase, also increases with the magnetic field. When the sample had a good coupling it was able to dissipate the energy coming from small phase changes within the sample, whereas bad couplings make the released heat remaining in the sample become reabsorbed and results in avalanches.

Another easy way to vary the thermal coupling between the sample and the bath is to change the ratio volume–surface of the samples. It is expected that the small sample would better thermalize during the field sweep as the dissipating term is increased, whereas the reaction is not modified. Figure 5(b) shows magnetization curves at 2.5 K for two samples (LPCMO(0.4)) which differ considerably in size. The large one had a volume $V \sim 1 \text{ m}^3$ whereas the smaller was $V \sim 0.3 \text{ m}^3$. The ratio volume–surface of the first sample was about three times larger than the smaller one. Samples were zero field cooled at a rate of 10 K min^{-1} until the desired temperature and then a magnetic sweep field of 1000 Oe/step applied. We observe the smaller sample jumping at a larger magnetic field, which support the idea that bad thermal couplings enhance the ignition of avalanches.

In summary, we have performed a qualitative study of the ignition of the abrupt phase avalanches in $\text{La}_{5/8-y}\text{Pr}_y\text{Ca}_{3/8}\text{MnO}_3$ emphasizing the role of the thermal coupling. The necessary conditions to produce the instability effect have been analyzed. Such an instability has been described in a reaction–diffusion system for the sample temperature. The experiments

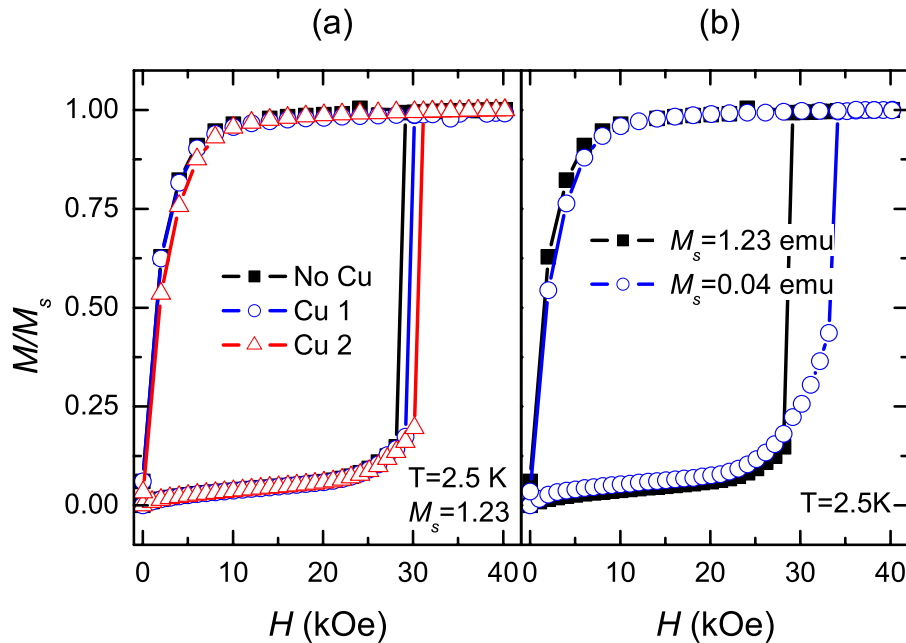


Figure 5. Isothermal magnetization curves measured under different conditions (LPCMO(0.4)). In (a) three curves with different sample holders, black squares for the plastic holder, blue circles for a sample in contact with a piece of a 2 mm copper wire and red triangles for a sample completely wrapped with a 0.1 mm copper wire. In (b) there are two curves corresponding to samples with very different sizes, in black squares a sample with $M_s = 1.23$ emu and in blue triangles a sample with $M_s = 0.04$ emu.

show that bad thermal couplings allow samples to be out of equilibrium and generate the avalanche instability process faster and more easily than well thermalized samples. With these data we have elucidate some physical questions related to the ignition of sharp steps or avalanches involving heat release. It is now possible to review many similar processes in different manganites and, probably, to extrapolate the results to a large set of other materials showing similar fast transitions involving heat propagation.

Acknowledgments

This work was supported by contract MAT2005-06162 from the Spanish Ministerio de Educación y Ciencia (MEyC). FM thanks the MEyC for a research grant. JMH thanks the MEyC and the Universitat de Barcelona for a Ramón y Cajal research contract. JT thanks ICREA for an ICREA ACADEMIA award. The authors also thank Francisco Parisi and Gabriela Leyva for preparing and providing samples.

References

- [1] Dagotto E 2005 *Science* **309** 257
- [2] Moreo A, Yunoki A and Dagotto E 1999 *Science* **283** 2034
- [3] Ghivelder L and Parisi F 2005 *Phys. Rev. B* **71** 184425
- [4] Hardy V, Maignan A, Hébert S, Yaïcle C, Martin C, Hervieu M, Lees M R, Rowlands G, Paul D Mc K and Raveau B 2003 Observation of spontaneous magnetization jumps in manganites *Phys. Rev. B* **68** 220402
- [5] Ghivelder L, Freitas R S, das Virgens M G, Continentino M A, Martinho H, Granja L, Quintero M, Leyva G, Levy P and Parisi F 2004 *Phys. Rev. B* **69** 214414
- [6] Hardy V, Majumdar S, Crowe S J, Lees M R, Paul D Mc K, Hervé L, Maignan A, Hébert S, Martin C, Yaïcle C, Hervieu M and Raveau B 2004 *Phys. Rev. B* **69** 020407
- [7] Liao D Q, Sun Y, Yang R F, Li Q A and Cheng Z H 2006 *Phys. Rev. B* **74** 174434
- [8] Rana D S, Kuberkar D G and Malik S K 2006 *Phys. Rev. B* **73** 064407
- [9] Fisher L M, Kalinov A V, Voloshin I F, Babushkina N A, Khomskii D I, Zhang Y and Palstra T T M 2004 *Phys. Rev. B* **70** 212411
- [10] Macià F, Hernández-Mínguez A, Abril G, Hernandez J M, García-Santiago A, Tejada J, Parisi F and Santos P V 2007 *Phys. Rev. B* **76** 174424
- [11] Jin S, Tiefel T H, McCormack M, Fastnacht R A, Ramesh R and Chen L H 1994 *Science* **264** 413
- [12] Parisi F, Levy P, Ghivelder L, Polla G and Vega D 2001 *Phys. Rev. B* **63** 44419
- [13] von Helmolt R, Wecker J, Holzapfel B, Schultz L and Samwer K 1993 *Phys. Rev. Lett.* **71** 2331
- [14] Macià F, Abril G, Hernández-Mínguez A, Hernandez J M, Tejada J and Parisi F 2008 *Phys. Rev. B* **77** 012403
- [15] Strykowski E and Giordano N 1977 *Adv. Phys.* **26** 487
- [16] Suzuki Y, Sarachik M P, Chudnovsky E M, McHugh S, Gonzalez-Rubio R, Avraham N, Myasoedov Y, Zeldov E, Shtrikman H, Chakov N E and Christou G 2005 *Phys. Rev. Lett.* **95** 147201
- [17] Hernández-Mínguez A, Hernandez J M, Macià F, Garcia-Santiago A, Tejada J and Santos P V 2005 *Phys. Rev. Lett.* **95** 217205
- [18] Maignan A, Hébert S, Hardy V, Martin C, Hervieu M and Raveau B 2002 *J. Phys.: Condens. Matter* **14** 11809
- [19] Mahendiran R, Maignan A, Hébert S, Martin C, Hervieu M, Raveau B, Mitchell J F and Schiffer P 2002 *Phys. Rev. Lett.* **89** 286602
- [20] Hébert S, Hardy V, Maignan A, Mahendiran R, Hervieu M, Martin C and Raveau B 2002 *J. Solid State Phys.* **165** 6–11
- [21] Hardy V, Hébert S, Maignan A, Martin C, Hervieu M and Raveau B 2003 *J. Magn. Magn. Mater.* **264** 183
- [22] Yaïcle C, Frontera C, García-Muñoz J L, Martin C, Maignan A, André G, Bourée F, Ritter C and Margiolaki I 2006 *Phys. Rev. B* **74** 144406
- [23] Woodward F, Lynn J, Stone M, Mahendiran R, Schiffer P, Mitchell J, Argyriou D N and Chapon L C 2004 *Phys. Rev. B* **70** 174433

- [24] Webster C H, Kazakova O, Gallop J C, Josephs-Franks P W, Hernández-Mínguez A and Tzalenchuk A Ya 2007 *Phys. Rev. B* **76** 012403
- [25] Sacanell J, Parisi F, Campoy J C P and Ghivelder L 2006 *Phys. Rev. B* **73** 014403
- [26] Hernández-Mínguez A, Macià F, Hernandez J M, Tejada J and Santos P V 2008 *J. Magn. Magn. Mater.* **320** 1457
- [27] McHugh S, Jaafar R, Sarachik M P, Myasoedov Y, Finkler A, Shtrikman H, Zeldov E, Bagai R and Christou G 2007 *Phys. Rev. B* **76** 172410
- [28] Pomjakushin V Yu, Sheptyakov D V, Conder K, Pomjakushina E V and Balagurov A M 2007 *Phys. Rev. B* **75** 054410
- [29] Chudnovsky E M and Garanin D A 2007 *Phys. Rev. B* **76** 054410